Enhancing Solubility, Stability, and Catalytic Properties of Human Paraoxonase-1 for Use as a Therapeutic Agent in Organophosphorus Poisoning

A Senior Honors Thesis

Presented in Partial Fulfillment of the Requirements for graduation with research distinction in the undergraduate colleges of The Ohio State University

by

Kathryn Hoffman

The Ohio State University
May 2011

Project Advisor: Thomas J. Magliery

Committee:
Dr. Thomas J. Magliery
Dr. Christopher M. Hadad
Dr. Nicole Cartwright Kwiek

Abstract

Organophosphorus compounds (OPs) are inhibitors of acetylcholinesterase. OPs are used in certain pesticides and are used in chemical warfare as nerve agents. Paraoxonase-1(PON1) is a serum hydrolase that naturally hydrolyzes OPs and could potentially be used as a therapeutic against OP poisoning. However, PON1 is not very soluble, stable, or active against OP substrates. PON1 has three cysteines, two of which form a disulfide in the folded form, which makes the protein more susceptible to misfolding with oxidation or disulfide scrambling. Many recombinant forms of PON1 (rePON1) have been made which enhance the solubility and expressibility of the enzyme (e.g. G3C9 and G2E6). In order to better understand the active site of the enzyme, a series of mutations near the active site were made in the G3C9 active site and tested for activity against paraoxon; phenylacetate; and a lab analog of G-nerve agents, CMP. Also, variants of the rePON1 have been engineered by Tawfik et al. that increase the catalytic efficiency of the enzyme (e.g. 4E9). In order to maintain the catalytic efficiency of 4E9 and simplify PON1 production, two different cysteine modified mutants were made to 4E9. These mutants were made by overlap PCR methods along with standard cloning techniques. In order to maintain the catalytic efficiency of 4E9 but also make the enzyme more human-like, a gene was designed that has the 4E9 active site and only the surface polar mutations of G2E6. All three variants were expressed and purified by Ni-NTA affinity column chromatography. The activities of the variants are tested against various OP substrates such as paraoxon and a lab analog of G-nerve agents, CMP. The results showed that the engineered variants proved to have similar activity to the parent, less drug-like molecules.

Dedication

Dedicated to my parents, Gary and Nancy Hoffman for all of their love and support.

Acknowledgments

Thomas J. Magliery- Principal Investigator/Advisor- Ohio State University Departments of Chemistry and Biochemistry

Christopher Hadad- Oral Exam Committee- Ohio State University Department of Chemistry

Nicole Cartwright Kwiek- Oral Exam Committee- Ohio State College of Pharmacy

Christina K. Harsch- Chemistry Graduate Student

David Mata- Chemistry Graduate Student

Vivekanand Shete- Postdoctoral Associate

Mohosin Sarkar- Postdoctoral Associate

Natasha Bharwani- Undergraduate Student

All members of Magliery Lab for their help and guidance.

Funding

College of Pharmaceutical Sciences Undergraduate Research Scholarship

University Honors and Scholars Center Honors Summer Research Scholarship

NIH- U54NS0581183 Research Grant

Vita

2007	Fairfield High School, Fairfield, Ohio
2009-2011	Undergraduate Researcher, Department of Chemistry and Biochemistry, The Ohio State University

Fields of Study

Major Fields: Pharmaceutical Sciences and Chemistry

Area of Distinction: Chemistry

Table of Contents

Introduction:

Organophosphorus Background

Organophosphorus compounds (OPs) are among the most toxic identified substances.[1] Across the developing world, acute OP pesticide poisoning causes tens of thousands of deaths each year.[2] Originally, OPs were developed for use as pesticides or insecticides,[3] but their extreme toxicity toward vertebrates has led to their use as chemical nerve agent weapons of mass destruction. OPs act as an indirect cholinergic agonist by irreversibly binding to the catalytic serine residue of acetylcholinesterase to prevent the breakdown of acetylcholine in the synaptic cleft.[4]

Acetylcholine is a neurotransmitter of the central and peripheral nervous system and functions as a neuromodulator. In the central nervous system, acetylcholine is released at the skeletal myoneural junctions.[5] In the autonomic subdivision of the peripheral nervous system, acetylcholine is the principle neurotransmitter released by the terminal nerve endings of all postganglionic, parasympathetic nerves and in both sympathetic and parasympathetic ganglia. Acetylcholine binds to the nicotinic and muscarinic acetylcholine receptors.[5] The overstimulation of these receptors, caused by the inhibition of acetylcholinesterase, can lead to muscarinic and nicotinic effects. Muscarinic effects include bradycardia, hypotension, rhinorrhea, bronchorrhea, bronchospasm, cough, increased salivation, nausea and vomiting, abdominal pain, diarrhea, fecal incontinence, urinary incontinence, blurred vision, increased lacrimation, miosis, and excessive sweating.[5] Nicotinic effects include tachycardia, hypotension, weakness, cramps, and paralysis.[5]

As of now, OP poisoning is treated post-exposure with a cholinergic antagonist or oximes. Atropine is an example of a cholinergic antagonist that binds to the muscarinic

acetylcholine receptor to prevent the overstimulation by acetylcholine.[5] Atropine does not prevent the binding of OPs to acetylcholinesterase and does not address the source of the poisoning. Oximes are strong nucleophilic agents that are known to reactivate the phosphorylated acetylcholinesterase by binding to the OP molecule. After exposure to select OPs, reactivation has been shown to be complete when oximes are administered one hour after exposure, but the effects are different with different OPs.[5,6] In moderate and severe cases of OP poisoning, oximes appear to have no effect and do more harm than good.[5,6] Both Atropine and oximes are post-exposure treatments to OP poisoning, but reaching the OP agent before it arrives at the synapse could be a more efficient therapeutic method.

The enzymatic inactivation of OPs has been suggested as a therapeutic strategy. The goal is to engineer a recombinant human protein to act as a therapeutic biological scavenger that would be able to reduce the OP concentration in affected blood.[7] The target proteins known to have potential therapeutic properties against OPs are the human organophosphorous acid anhydride hydrolases (OPAHs), including human paraoxonase (huPON) and human butyrylcholinesterase.[8]

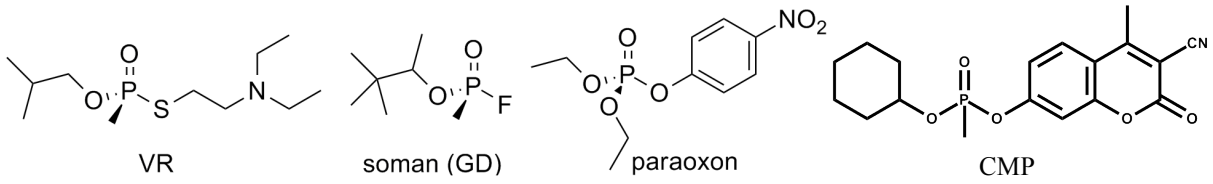

Figure 1: Above are the molecular structures of two examples of nerve agents, VR and soman, and an example of an OP that is a metabolite of the pesticide parathione, paraoxon. A lab analog of G-agents, CMP, is also shown in the figure above.

Therapeutic Agents

Human butyrylcholinesterase (HuBChE) has been produced as a scavenger. HuBChE parallels synaptic acetylcholinesterase[9] in primary amino acid sequence, deduced secondary structure, and active site chemistry; the two enzymes also have overlapping specificity for substrates and inhibitors. One of the limitation of this bioscavenger is its stoichiometric (1:1 ratio) nature of binding to nerve agents, requiring large amount of HuBChE (60 mg/kg in guinea pigs) for in vivo protection against 2 - 5 LD_{50} nerve agent exposure.[10, 11, 12, 13, 14] Progress has been made in converting butyrylcholinesterase into a "catalytic scavenger" by changing the glycine at position 117 to a histidine in order to fuel the hydrolysis of the OP through an acid-base mechanism.[15] The affinity and catalytic activity of the mutant are lower than that of human paraoxonase-1 (huPON1).[15]

PON1 is one of three members of the PON family. PON1 and PON3 both associate with high density lipoprotein (HDL). Both proteins are capable of protecting low-density lipoproteins (LDL) against oxidative stress, reducing macrophage foam cell formation and preventing atherosclerosis development.[16, 17] PON2 is expressed in nearly all tissues and does not associate with HDL particles in circulation. The PON family has been involved in the reduction of oxidative stress and the protection against atherosclerosis.[16, 17] Furthermore, the ability of PON1 to enzymatically hydrolyze OPs makes PON1 a protein of interest as a potential bioscavenger.

Human Paraoxonase-1

HuPON1 is a serum-based, calcium-dependent enzyme that is mainly synthesized in the liver. PON1 exists in different polymorphic forms. The two common isoforms that have been extensively studied contain polymorphisms at position 55 and 192.[14, 18, 19, 20] The former

influence the expression level of PON1 and the latter affects the enzymatic activity. PON1 polymorphism in the promoter region is reported to influence the level of protein expression.[20] The physiological role of PON1 is still unclear, but evidence exists for its protective effect against oxidative modifications of lipoproteins.[14, 17, 22, 23, 24] The crystal structure of huPON1 has not been solved; however, the crystal structure of a recombinant version, G2E6, which hydrolyzes esters including lactones and OPs has been solved.

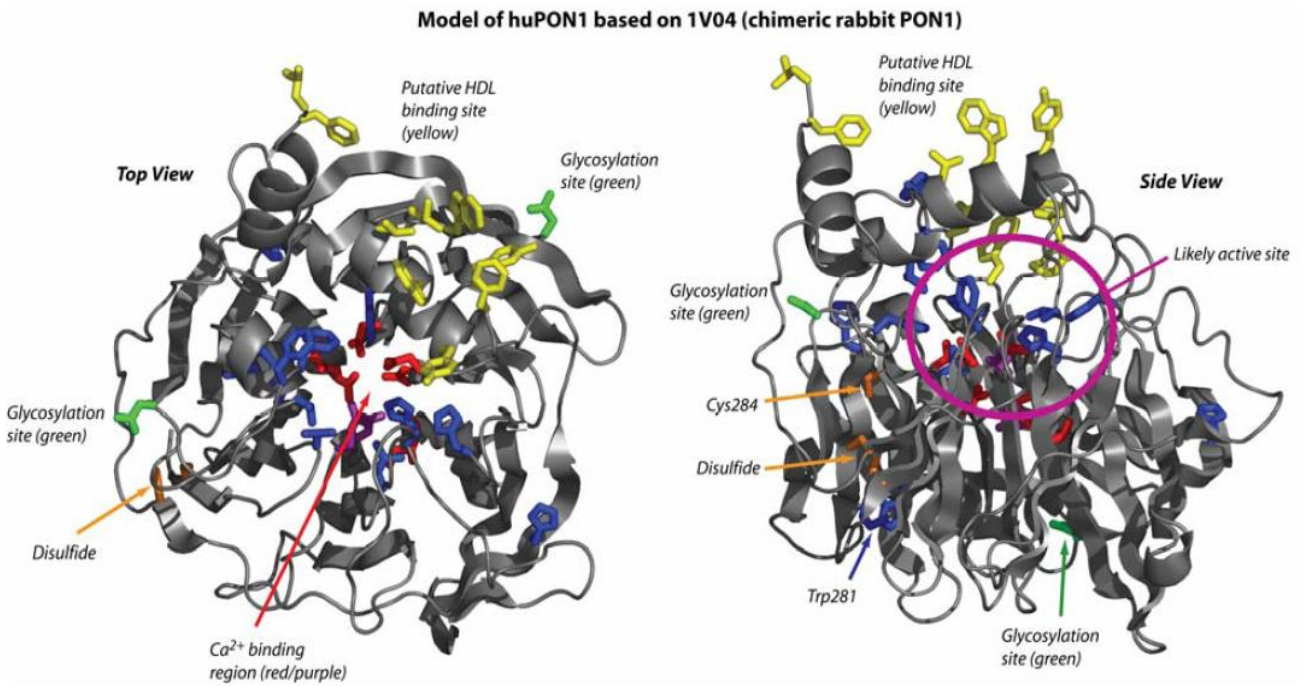

Figure 2: Model of the structure of huPON1 based on the X-ray crystal structure of a chimeric rabbit PON1 variant. Important residues are rendered as sticks and colored for: Ca^{2+} binding (red and purple); putative sites of glycosylation (green); cysteines (orange); and putative site of HDL binding (yellow). Blue and purple residues have been found to affect the activity or specificity of PON1 in derivatization, mutational or evolutionary studies. The preponderance of the activity and structural evidence suggests that the active site lies in a pocket just above (and probably including) the Ca^{2+} binding site in the middle of the -barrel. The model was generated with SwissModel from PDB entry 1V04, and the figure was generated with PyMOL.
*This figure and caption were taken from the proposal by Sayre, Magliery, & Wang.

There are some difficulties associated with using huPON1 therapeutically. First, it must be cheaply generated in large amounts without any contaminations of immunogens or pathogens from the vector organism. Second, PON1 has three cysteines, two that form a disulfide bond in

the folded form which makes the protein more susceptible to misfolding upon oxidation or disulfide scrambling. Third, its affinity for and turnover of nerve agents are weak.[25,26] Fourth, huPON1 is not very stable and is not easily expressed.[27] Efforts to improve huPON1 activity toward OPs are severely restricted by an incomplete understanding of the active site and mechanism.

If recombinant PON1 (rePON1) variants are made that are very similar to huPON1 as well as soluble and expressible in *E. coli*, we will be able to better understand the location of its active site and the mechanisms it undergoes. Efforts have previously been made to enhance the expressibility of PON1. Tawfik and coworkers used DNA shuffling and activity screening to obtain the first PON1 variants that express in a soluble and active form in *E. coli*. One variant in particular, G3C9, yielded over 12 mg/liter culture of pure, active, unmodified PON1.[16]

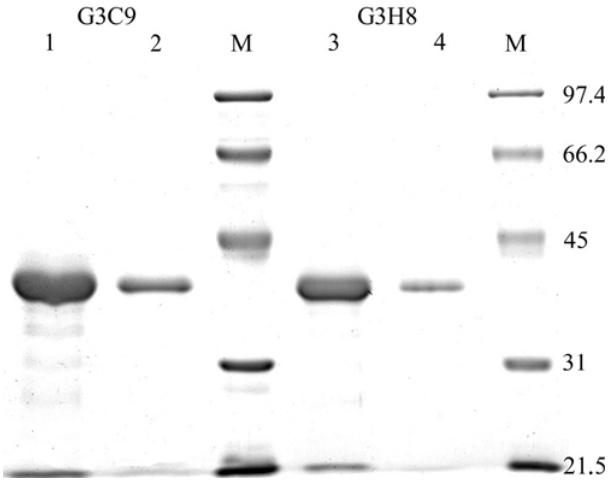

Figure 3: An SDS-PAGE gel showing two of the most expressible and soluble variants found, G3C9 and G3H8.[16]

	Phenylacetate hydrolysis			Paraoxon hydrolysis			Yield, purified enzyme
Variant*	k_{cat}, s^{-1}	K_M, mM	k_{cat}/K_M, $M^{-1}\,s^{-1}$	k_{cat}, s^{-1}	K_M, mM	k_{cat}/K_M, $M^{-1}\,s^{-1}$	mg/liter culture
G1A5†	833	0.39	2.1×10^6	1.16	0.085	1.4×10^4	2.2
G1C4†	552	0.54	1.0×10^6	0.54	0.12	0.5×10^4	2.7
G2D6†	562	0.32	1.7×10^6	0.98	0.10	1.4×10^4	14.4
G2E6†	965	0.43	2.2×10^6	0.87	0.089	1.0×10^4	20
G3H8‡	1018	0.32	3.2×10^6	1.2	0.088	1.4×10^4	11.8
G3C9‡	789	0.33	2.4×10^6	1.1	0.094	1.2×10^4	12.6
Wild-type HuPON1§	1236	0.42	2.9×10^6	3	0.54	0.6×10^4	0

Table 1: A comparison of the enzymatic activity of the variants made. All of the variants that are shown in the table maintained similar activity to the wild-type huPON1 against paraoxon and phenylacetate.[16]

The rePON1, G3C9, variant has been used in structural and mechanistic studies because it, unlike huPON1, is soluble and expressible in *E. coli.*[16] Bacterial expression enables compatibility to semi-rationally improve the properties of PON1. We can carry out mutagenic studies on the soluble rePON1, G3C9 variant; however, the protein sequence is not very similar to the human homolog. Therefore, it would be quite useful to engineer a soluble, *E. coli* expressible, PON1 variant that is a near-variant of the human homolog. Manufacturing huPON1 variants for *E. coli* expression is necessary for improving its stability and ablating unfavorable properties. It would also be useful to involve a more efficient active site in the protein.

Solubility and Active Site Modifications

Fusion of a seemingly insoluble protein with more soluble bacterial proteins helps increase the solubility and expression levels of the test proteins.[27, 28] Glutathione S-transferase (GST), thioredoxin (Trx) and Maltose Binding Protein (MBP) have been successfully applied as a fusion protein to increase the solubility and expressibility of a number of difficult-to-express proteins or human proteins.[28, 29] (M311, 312) MBP has proven to be a better fusion partner to express protein with better solubility and higher yields.[27, 28]

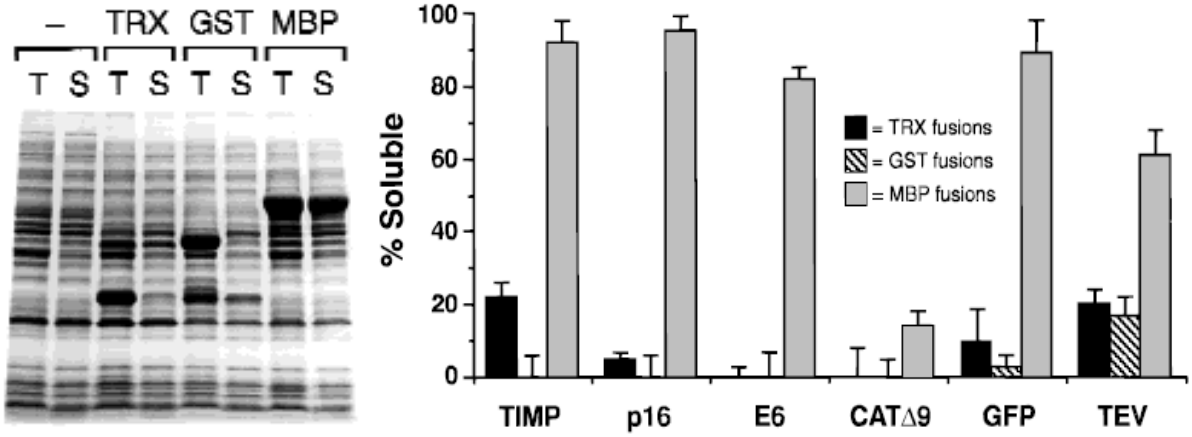

Figure 4: A gel and chart summarizing the findings of Kapust et al. The SDS PAGE gel is of the generally insoluble protein, TIMP, fused with TRX, GST, or MBP. The gel shows that fusing an aggregation-prone protein to any highly soluble partner will routinely give rise to a soluble fusion protein. The chart illustrates that MBP is a much better solubilizing agent than GST or TRX MBP fusion.

A PON1 variant has been designed to increase the stability and solubility of huPON1. The variant incorporated changes in perceived surface residues of huPON1 that changed the residues to the more polar residue found at that position on the G2E6 rePON1. The variant was termed G2E6 polar (G2E6p). A total of 15 changes (I5T, N19R, Q21K, L31H, N78D, N80D, S81K, P82S, L96S, G101E, A137S, N166S, Q192K, Y197H, N265D and N309D) were made to the surface of PON1, which is less than the 59 residual variations between G2E6 and huPON1 or the 51 residual variations between G3C9 and huPON1.[28] As a fusing to folding reporter green fluorescent protein (frGFP), Mohosin Sarkar was able to use fluorescent screening to show that G2E6p is more soluble than huPON1.[28] frGFP distinguishes proteins that fold robustly and are highly soluble from those which aggregate. It has been observed that the solubility of a protein is directly correlated to the fluorescence of the cell.[28]

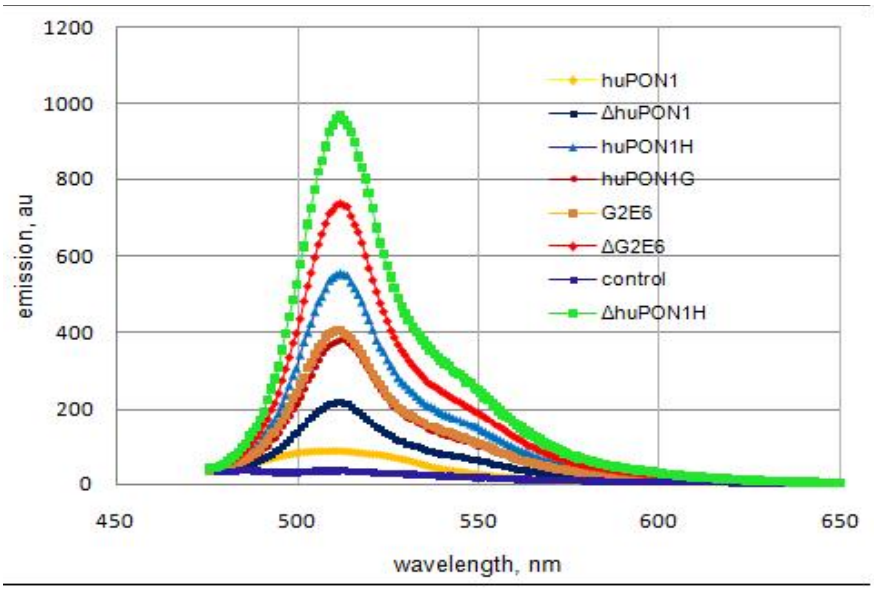

Figure 5: Fluorescent diagram showing huPON1 and G2E6p (labeled huPON1G) as well as some other variants. G2E6p or huPON1G is more fluorescent than huPON1.

Recently, Dan Tawfik and coworkers used both applied and targeted mutagenesis to rePON1 and screened the mutants for organophosphate hydrolysis using both high-throughput fluorescence-activated cell sorting (FACS) screening and low-throughput plate screening. One of the variants reported, 4E9, had increased enzymatic efficiency against the more toxic, S_p, isomer of the nerve agent analog, CMP (shown in **Figure 1**).[29] 4E9 varies from G3C9 in 6 positions (L69G, S111T, H115W, H134R, F222S, T332S), all of which are located in the putative active site of PON1.[29]

		S_p-CMP-coumarin[c]			R_p-CMP-coumarin	S_p-CMP-F
Variant[a]	Mutations[b]	k_{cat} (min^{-1})	K_M (μM)	k_{cat}/K_M ($\mu M^{-1}\ min^{-1}$)	Apparent k_{cat}/K_M[c] ($\mu M^{-1}\ min^{-1}$)	Apparent k_{cat}/K_M[c] ($\mu M^{-1}\ min^{-1}$)
rePON1-G3C9	(Wild-type-like)	ND	ND	<0.0002 (1)[d]	0.08 ± 0.003 (1)	0.13 ± 0.03 (1)
3B3	N41D, S110P, **L240S**, H243R, F264L, N324D, **T332A**	ND	ND	<0.0002 (1)[d]	20 ± 2 (250)	~0.0001
H115W-V346A	**H115W**, **V346A**	ND	ND	0.0013 ± 0.0005 (>6)	0.4 ± 0.01 (5)	0.018 ± 0.002 (0.14)
3A7	V97A, **H115W**, P135A, **F222S**, M289I	ND	ND	0.003 ± 0.0005 (>15)	0.16 ± 0.008 (2)	0.011 ± 0.004 (0.08)
8C8	**L69S**, V97A, **H115W**, P135A, **F222S**	15.1 ± 2	84.5 ± 16	0.18 ± 0.02 (>900)	–[e]	0.15 ± 0.05 (1.1)
2D8	**L69G**, **H115W**, **H134R**, **F222S**, **T332S**	395 ± 23	42.5 ± 5	9.3 ± 0.6 (>46000)	–[e]	4.65 ± 0.1 (36)
3D8	**L69G**, **H115W**, **H134R**, M196V **F222S**, **T332S**	546 ± 29	36.7 ± 7	12.7 ± 2 (>63,000)	–[e]	3.14 ± 0.5 (24)
4E9	**L69G**, S111T, **H115W**, **H134R**, **F222S**, **T332S**	540 ± 37	32.8 ± 10	17.3 ± 4 (>86,000)	–[e]	17.5 ± 3 (135)

Table 2: This table summarizes the findings of Tawfik et al. from the fluorescence-activated cell sorting screening. Two interesting findings include 3B3 having most to all activity against the R_p, or less toxic isomer, and 4E9 has high activity against the S_p, or more toxic isomer.[29]

In order to design a more humanlike variant with increased enzymatic efficiency, we designed a gene containing both sets of mutations in the huPON1 scaffold. This would increase the solubility of the human protein while hopefully maintaining the activity or enzymatic efficiency associated with 4E9. The resulting gene was termed 4E9 polar (4E9p). The gene includes 2 other residual mutations (A125T, V206T) that were not included when designing G2E6p. The gene exists both fused to MBP and without MBP.

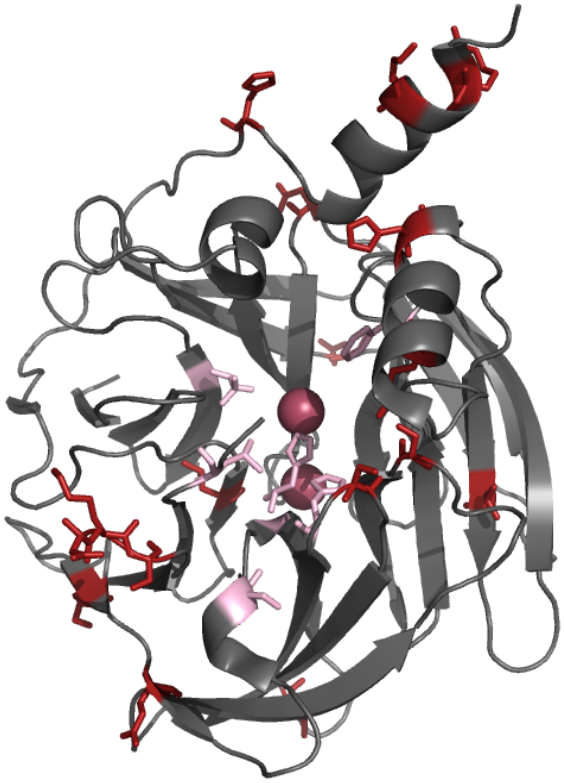

Figure 6: The structure of rePON1 with the residual differences between huPON1 and 4E9p highlighted in red (if it is a surface mutation obtained from G2E6) and pink (if it is an active site mutation obtained from 4E9).

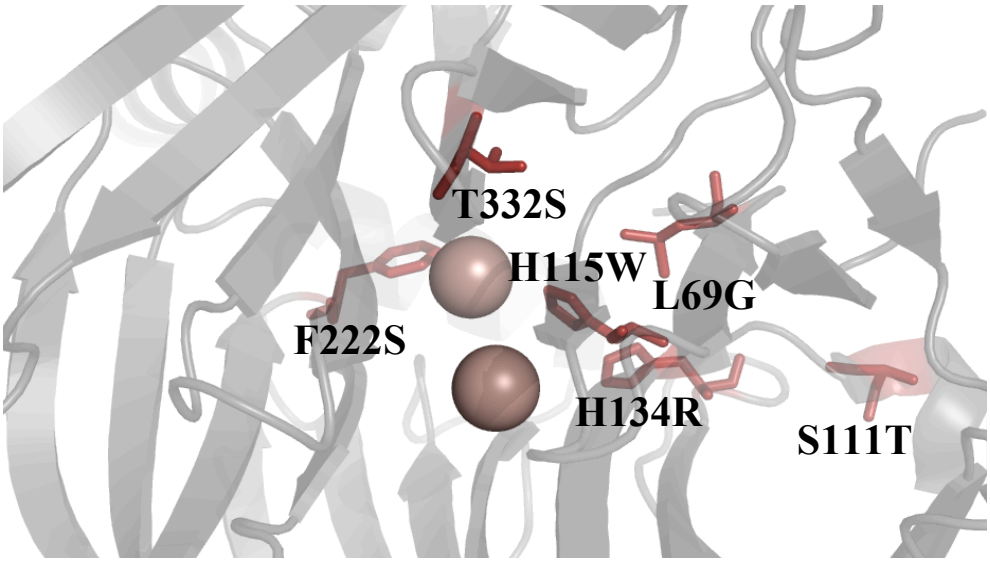

Figure 7: Putative active site of rePON1 with the changed residues between G3C9 and 4E9 highlighted and labeled.

Cysteine Modifications

PON1 has three cysteines (at positions 42, 283, and 353), two of which form a disulfide in the folded form (42-353). Cysteine residues can complicate the folding and storage of proteins due to improper formation of disulfide bonds or oxidation of reduced residues.[30, 31] Oxidation can lead to changes in the physicochemical properties of a protein.[30] These modifications range from changes in hydrophobicity and isoelectric point to conformational changes.[30] Also, oxidation is a potential problem in protein production, isolation, and purification processes.[30] Mutating cysteines to residues that are similar in size and shape such as alanine or valine can still yield a protein with similar folding and kinetic properties as the wild type. For example, Sanjay Hari and colleagues mutated the two cysteines (C38 and C52) of the protein Rop and concluded that the C38A C52V variant of Rop is active, has wild-type like thermal stability, exhibits a cooperative thermal denaturation, and has similar although slightly reduced stability to urea denaturation.[30]

It would be preferable to have a therapeutic version of huPON1 that is Cys-free (or at least have only 1-2 Cys) without affecting the activity or folding of the enzyme. An experiment was executed using G2E6 as the scaffold in which a variety of cysteine (Cys) mutation combinations were changed to alanine (Ala) or valine (Val).[32] The table below summarizes the activity findings using phenyl acetate as the substrate.

S—S SH 42	283	353	k_{cat}/K_m (K_m)	↑↓
Cys	Cys	Cys	203 (0.6)	-
Cys	Ala	Cys	65 (0.8)	0.3
Cys	Val	Cys	330 (1.1)	1.6
Ala	Cys	Cys	120 (1.1)	0.6
Val	Cys	Cys	53 (1.1)	0.3
Cys	Cys	Ala	99 (0.8)	0.5
Cys	Cys	Val	218 (1.6)	1.07
Ala	Cys	Val	373 (0.7)	1.84
Val	Cys	Ala	98 (0.7)	0.5
Ala	Val	Val	19 (0.7)	0.1
Ala	Ala	Val	130 (0.6)	0.6

Table 3: This table shows the variations in kcat/Km in mM^{-1} min^{-1} among the different mutants using phenyl acetate as the substrate.[32]

The results concluded that the C42A and C353V (ACV) and C283V (CVC) mutants maintained similar activity to wild type. These two mutants were screened for activity under oxidizing conditions to yield the results shown in the figure below.

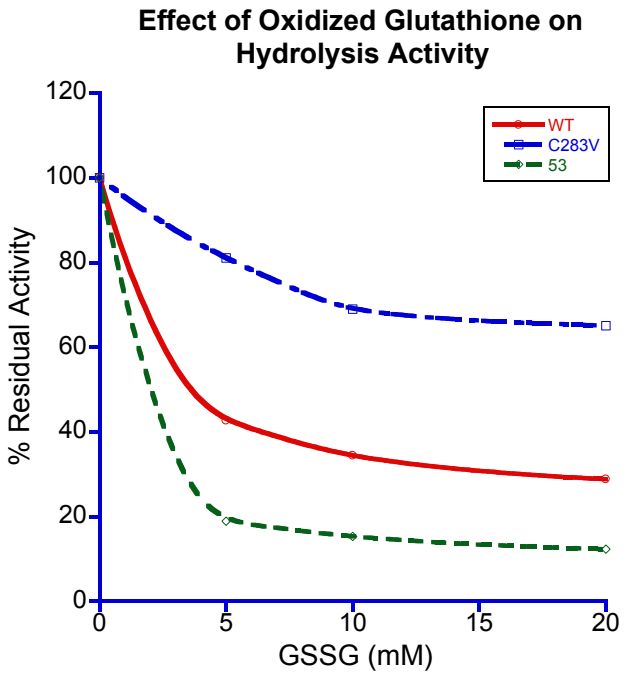

Figure 8: A graph showing the % Residual Activity of CVC (blue), wild type (red), and ACV (green) against phenyl acetate versus various amounts of oxidizing agent (glutathione).[32]

The results showed that ACV and WT were susceptible to a loss in activity when under oxidizing conditions whereas CVC was not as susceptible to loss of function with increasing oxidizing agent.[32] The findings encouraged the design of both the ACV and CVC mutants in the 4E9 scaffold.

Figure 9: The structure of rePON1 highlighting the three cysteine residues. In pink is C283 and in red is C42 and C353. These two are responsible for forming a disulfide bond.

Materials and Methods:

Creation of Cys-free and G3C9 mutants

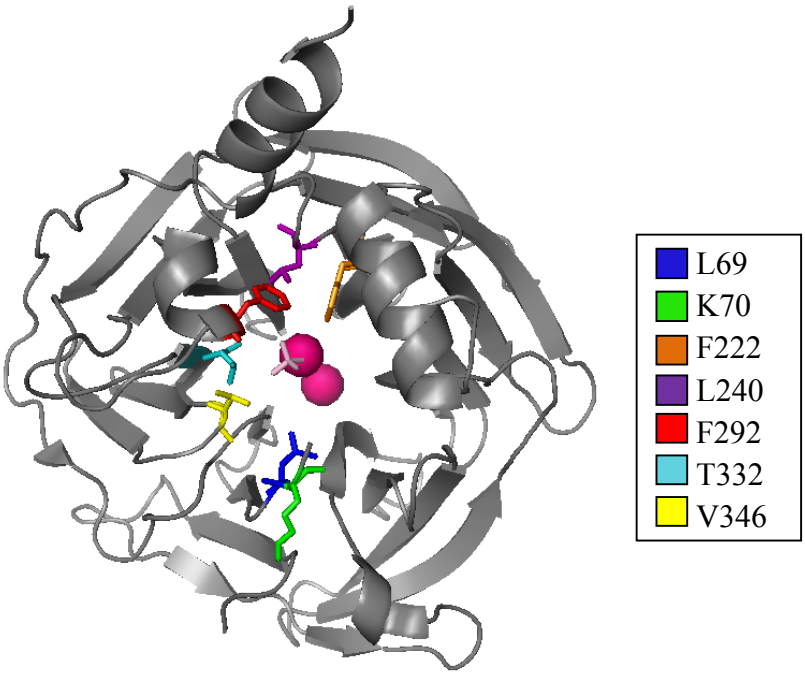

Figure 10: Structure of rePON1 highlighting the residues mutated in G3C9.

Variants	Forward Mutagenic Primers	Reverse Mutagenic Primers
C42A	AAC TCC AGT GGA ACT TCC TAA CGC TAA TTT AGT TAA AGG GGT TGA C	GTC AAC CCC TTT AAC TAA ATT AGC GTT AGG AAG TTC CAC TGG AGT T
L69G*	GGC TTT CAT CAG CTC CGG AGG TAA GTA TCC TGG AAT AAT GAG	CTC ATT ATT CCA GGA TAC TTA CCT CCG GAG CTG ATG AAA GCC
L69S	GGC TTT CAT CAG CTC CGG ATC AAA GTA TCC TGG AAT AAT GAG	CTC ATT ATT CCA GGA TAC TTA GAT CCG GAG CTG ATG AAA GCC
K70A*	CTT TCA TCA GCT CCG GAT TAG CAT ACC CTG GAA TAA TGA GCT	AGC TCA TTA TTC CAG GGT ATG CTA ATC CGG AGC TGA TGA AAG
F222S	GCA GAA GGA TTT GAC TCA GCT AAC GGA ATC AAC ATC TCA	GAT GTT GAT TCC GTT AGC TGA GTC AAA TCC TTC TGC TCG
L240S	GTA TGT CTA TAT AGC TGA GTC GCT GGC TCA TAA GAT CCA TG	CAT GGA TCT TAT GAG CCA GCG ACT CAG CTA TAT AGA CAT AC
C283V	AGG GGA TCT CTG GGT TGG TGT ACA TCC TAA CGG AAT GCG AAT C	GAT TCG CAT TCC GTT AGG ATG TAC ACC AAC CCA GAG ATC CCC
F292A	CCC AAC GGA ATG CGA ATT GCC TAC TAT GAC CCA AAG AAT C	GAT TCT TTG GGT CAT AGT AGG CAA TTC GCA TTC CGT TGG GAT G
T332A*	TGG CAC TGT GTT ACA GGG AAG AGC TGT GGC CGC TGT GTA CAA AG	CTT TGT ACA CAG CGG CCA CAG CTC TTC CCT GTA ACA CAG TGC CA

V346A	AAA CTG CTG ATT GGC ACC GCG TTT CAC AAA GCT CTT TAC	GTA AAG AGC TTT GTG AAA CGC GGT GCC AAT CAG CAG TTT C
C353V	CAG TGT TTC ACA AAG CAC TTT ACG TTG AGC TGG CGG CCG CAC TCG	CGA GTG CGG CCG CCA GCT CAA CGT AAA GTG CTT TGT GAA ACA CTG

Table 4: This table gives the nucleic acid sequences for all the mutagenic primers used for cloning the G3C9 mutants as well as the Cys-free mutants in 4E9. Most of the mutants were cloned using Pfu polymerase. The mutants with * indicate that they were cloned using Herculase II polymerase.

Variants	Forward Cloning Primers	Reverse Cloning Primers
C42A, C353V, F292A, L69G, L69S, V346A	GTG AGC GGA TAA CAA CAA TTC CCC	CCA ACT CAG CTT CCT TTC GGG
K70A, F222S, T332A, L240A	GAT ATA CCC ATG GCT AAA CTG	AAT AAT GCT CGA GTG CGG CCG C
C283V (fragments)	GAG GGG TAA TAA TTA GTG GTG GTG GTG GTG GTG	TTA ACC GCA TTA ACT CTC TTG GGG CTG GGA TTG GCA C
C283V (overlap)	CTG CAC CAT CTC GAG GGG TAA TAA TTA GTG GTG GTG	GGT GGT GGC CCA TGG CTA AAT TAA CCG CAT TAA CTC TCT TGG

Table 5: This is a table of the cloning primers used to both complete the fragments for each mutant as well as to extend and amplify the overlap product.

Fragments were made doing a PCR reaction using the primers listed in the tables above. Once fragments were made, the fragments were joined/overlapped in a final PCR reaction to yield the final product. The final overlap product was then purified and digested using NcoI and XhoI. Below is a picture of a plasmid map of G3C9 with the cloning sites emphasized.

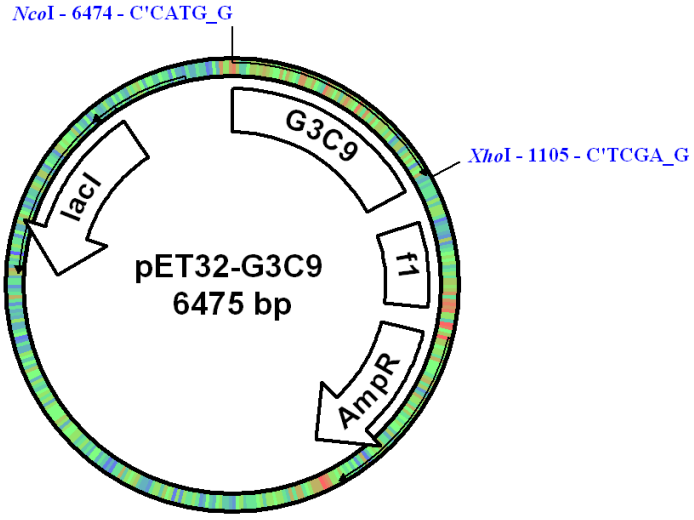

Figure 11: A plasmid map of G3C9 showing where the restriction enzymes used for cloning, NcoI and XhoI cut into the vector.

Creation of 4E9polar with and without MBP

In order to make 4E9 polar in the lab, it would require making several mutations to the DNA encoding the huPON1 gene. In order to remove this obstacle, the gene was synthesized by Genewiz (New Jersey). The amino acid sequence wanted for the gene was reverse translated using a back translation tool, which provided selective codon usage models for several different organisms. Due to the use of *E. coli* for protein expression purposes, *E. coli* was the species of choice for the codon usage model. Also, the four least common codons in *E. coli* (CTA, CCC, CGA, and AGG) were not permitted to be included in the gene. For cloning purposes, an NcoI site was placed at the beginning of the gene and an XhoI site was placed at the end of the gene. Also, two BamHI sites were placed at the very beginning and very end of the gene (originally cloned into the pUC57 vector. Due to the insoluble nature of the human protein, the gene initially was to be placed as a fusion to MBP in the pET11 vector. In order to move the gene into the pET11-MBP construct, both the pUC57 construct (containing the gene) and a pET11-MBP construct were digested using BamHI. The resulting insert and vector were purified using dialysis membrane and glass fiber filter paper. Then a ligation of the vector and insert was carried out using T4 ligase. The ligation reaction was transformed into DH10B via electroporesis and plated on LB AMP plates. The resulting colonies were analytically digested with SalI and EcoRV.

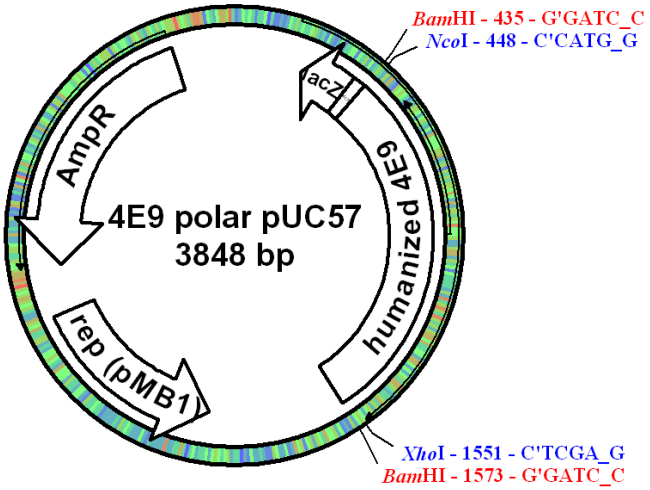

Figure 12: The original plasmid map of the gene received from the order in the pUC57 vector. The BamHI, NcoI, and XhoI sites are emphasized to show all the usable cloning sites of the designed gene.

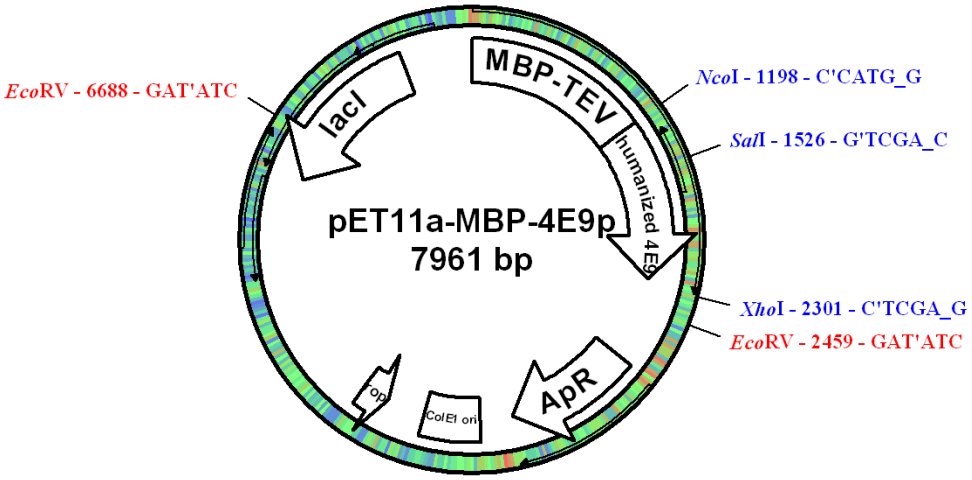

Figure 13: A plasmid map of the MBP fused protein showing the NcoI and XhoI sites that were used to make the gene without a fusion to MBP. Also emphasized are the analytical restriction sites of SalI and EcoRV.

In order to make the protein without the MBP fusion, the pET11-MBP-4E9 polar plasmid was cut with NcoI and XhoI and placed in the pET32 vector.

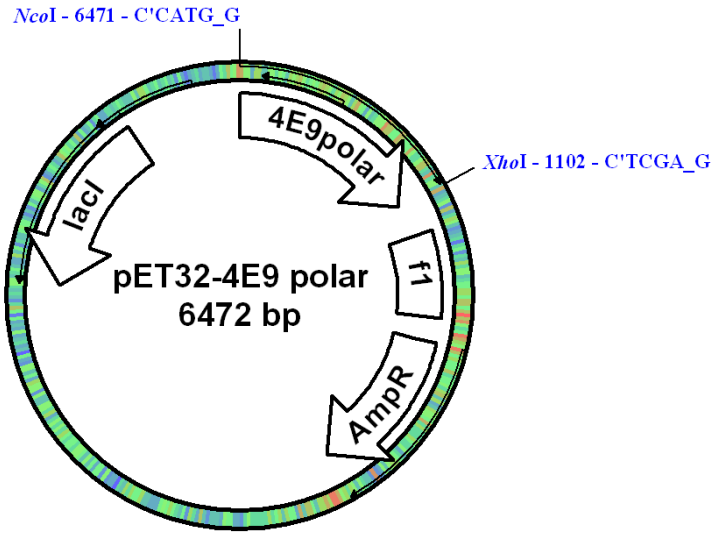

Figure 14: A plasmid map of 4E9 polar without MBP in the pET32 vector with the NcoI and XhoI cloning sites emphasized.

Purification and Expression of Variants:

All protein expression was carried out using the Origami B (DE3) strain of cells. Every G3C9 and Cys-free variant was expressed and purified using the same protocol. For all of those variants, the cell were grown at 37 °C until it reached an OD_{600} ~0.8. The samples were then induced using 0.1 mM isopropyl β-D-1-thiogalactopyranoside (IPTG) and placed at 30 °C for ~4 hours. The cells were then spun down to produce the pellet. The pellets were resuspended in ~45 mL lysis buffer (50 mM Tris pH 8, 1 mM $CaCl_2$, 50 mM NaCl, and 0.1 mM DTT). All of these variants were lysed on ice using a sonicator with the setting of 30 sec pulse, 2 minutes 30 sec pause, with a total pulse time of 3 minutes at a power of 6 W. For 4E9 polar, the cells were grown at 37 °C until it reached an OD_{600} of ~1 and induced using 0.3 mM IPTG at 16 °C overnight (~18 hours). The cells were centrifuged to obtain the pellet and the pellet was resuspended in ~45 mL lysis buffer. The 4E9 polar samples were lysed using an Emulsiflex to prevent over-heating of the protein. After lysing, 0.1% tergitol was added to all samples (Cys-

free and G3C9 variants included). The samples were then placed on a nutator at 4 °C for 2.5 hours. Equilibrated Ni-NTA resin (Qiagen) was added to the sample (0.3 mL per 1 L prep) and the samples were again placed on a nutator at 4 °C for ~3 hours to allow for the 6xHis tag located on the C-terminus of the protein to bind to the resin. The samples were then poured into a column and the table below describes the wash and elution buffers used to obtain the purified sample.

Activity buffer contains 50 mM Tris pH 8, 1 mM $CaCl_2$, 50 mM NaCl, and 0.1% Tergitol Protocol is for a 1 L prep of protein		
Buffer Name	**Imidazole Concentration**	**Volume Used**
Wash 1	10 mM	~45 mL
Wash 2	10 mM	~45 mL
Wash 3	25 mM	~25 mL
Elution 1	150 mM	~12 mL
Elution 2	150 mM	~15 mL

Table 6: This table summarizes the washing and eluting steps involved in Ni-NTA affinity chromatography protein purification

All samples were examined by SDS-PAGE to ensure protein concentration and level of purity. Elution 1 was then buffer exchanged twice using a dialysis cassette. The first exchange took place in activity buffer plus 10% glycerol (anywhere between 2-4 L is fine). The second exchange occurred in activity buffer plus 50% glycerol (again, anywhere between 2-4 L is fine). The reason buffer exchange took place is to remove imidazole from the sample as well as protect the protein sample from freezing for storage through the addition of glycerol to the sample. The samples were removed from the cassettes and stored at -20 °C.

Enzyme Kinetics and Assays

Prior to collecting kinetic data, the concentration of enzyme must be known. To determine the concentration of protein in a sample, a Bradford assay was used. A Bradford assay uses the Bradford reagent that changes color upon binding to protein. The color that the dye changes is observed at a wavelength of 595 nm. In order for a Bradford to effectively predict the concentration of protein in a sample, a calibration curve must be made using known concentration of protein. The calibration curve was done on the SpectraMax Plus 384 spectrophotometer using known concentration of Bovine Serum Albumin (BSA) ranging from 0.05-0.5 mg/mL. Various dilutions of enzyme were made until a dilution was found which fits within the calibration curve. The values were triplicated and a concentration can be determined. To confirm if the concentration is correct, the samples were normalized to 1 mg/ml and electrophoresed on an SDS gel with samples of BSA. Once protein concentration is determined, the enzyme is ready for kinetic studies.

Also, the concentration of substrate used must be known. The substrates paraoxon and phenyl acetate stock concentrations were confirmed through base hydrolysis. A strong base is added to a concentration of substrate that would give an absorbance value of 0.5. Depending on how off from 0.5, the absorbance values of the stock was adjusted to make up for the variation. To test the accuracy of the racemic CMP stock solution, the substrate is hydrolyzed using the rePON1, 3B3. 3B3 is known to hydrolyze only one of the two isomers. The final absorbance after hydrolysis is then used to calculate half the concentration of CMP in the stock. The stock concentration is then adjusted accordingly.

Below is a description of the substrate parameters used to test the activity of all the variants.

Paraoxon:

Final [Paraoxon] (mM)	Initial [Paraoxon] (mM)	Volume MeOH/mL (µL)	Volume Previous Stock/mL (µL)
2.6	130	973.0	27.0
1.8	90	307.7	692.3
1	50	444.4	555.6
0.52	26	480.0	520.0
0.26	13	500.0	500.0
0.13	6.5	500.0	500.0
0.06	3	538.5	461.5
0.03	1.5	500.0	500.0

Table 7: This table provides the concentrations of paraoxon used to collect the data points to fit the Michaelis-Menten curve. It also provides the amounts used to make each solution. The final concentration of MeOH is 2%.

Phenyl Acetate:

Final [Phenyl Acetate] (mM)	Initial [Phenyl Acetate] (mM)	Volume of MeOH (µL)	Volume of Previous Phenyl Acetate Stock (µL)
3.3	165	979.1	20.9
2.6	130	212.1	787.9
1.8	90	307.7	692.3
1.0	50	444.4	555.6
0.52	26	480.0	520.0
0.26	13	500.0	500.0
0.13	6.5	500.0	500.0
0.06	3	538.5	461.5

Table 8: This table provides the concentrations of phenyl acetate used to collect the data points to fit the Michaelis-Menten curve. It also provides the amounts used to make each solution. The final concentration of MeOH is 2%.

For paraoxon and phenyl acetate assays, 186 µL of assay buffer (50 mM Tris, 10 mM $CaCl_2$ pH 7.4), 10 µL of enzyme, and 4 µL of substrate (200 µL total reaction) are added in that order to the well. To determine the concentration of enzyme to be used, serial dilutions are made in one column of a 96 well plate (ranging from neat enzyme to a 1:128 dilution). The absorbance at 412 nm and 270 nm for paraoxon and phenyl acetate respectively was observed for 3-5

minutes with readings every 10 seconds. A dilution was chosen based on the linearity of the rate of absorbance of the leaving group and the dilution was used to triplicate the series. Using Beer's Law, the absorbance can be converted to concentration with a path length of 0.46 cm and the known extinction coefficients (ε) equal to17,000 M^{-1} cm^{-1} for paraoxon and 13,100 M^{-1} cm^{-1} for phenyl acetate.

CMP:

To test for CMP activity, enzymes were incubated in assay buffer with increasing concentrations of either CMP from 0.005mM to 0.5mM in a 96-well plate. In terms of volume, 146 μL of assay buffer, 50 μL of enzyme and 4 μL of substrate are added to the well. The rate of formation of the coumarin product was monitored at a wavelength of 405 nm (ε = 37,000 M^{-1} cm^{-1}) using SpectraMax Plus 384 spectrophotometer for 5-10 minutes. The stocks of CMP were prepared in MeOH, with a final concentration of 2% MeOH in the final reaction.

Another experiment was conducted to determine the activity of the enzyme against the more toxic, S isomer. As mentioned before, 3B3 turns over only one of the isomers, and it happens to be the less toxic isomer. To test for enzymatic activity against the more toxic isomer, 3B3 is incubated in assay buffer and 0.033 mM CMP. This reaction sits for 10-15 minutes so all of the less toxic isomer will be hydrolyzed and only the more toxic isomer will remain. The enzyme to be tested is added to this reaction to make the final concentration of CMP in solution 0.025 mM. Absorbance (at 405 nm) was observed over 10 second intervals for 5-10 minutes. A k_{cat}/K_m value can be extracted from the rate, substrate concentration and enzyme concentration.

All kinetic parameters were collected by Michaelis-Menten steady-state kinetics (See **Figure 15** for the equation). A Michaelis-Menten plot can be made by plotting the slope obtained

from the change in absorbance over time (converted to mM/min) versus the concentration of substrate used.

$$v_0 = \frac{V_{max}[S]}{K_m + [S]}$$

Figure 15: The equation above is the Michaelis-Menten equation. Where V_{max} is k_{cat} $[E]_t$. Experimentally, K_m is the concentration of substrate at half V_{max}. V_{max} is the horizontal asymptote the curve is constricted to.

The equation above can be manipulated depending on the concentration of substrate used. If the concentration of substrate is much smaller than the K_m, it is possible to extract the enzymatic efficiency (k_{cat}/K_m) by simply dividing the rate by the substrate and enzyme concentration. However, if the substrate concentration is much larger than the K_m value, it is possible to obtain the catalytic activity (k_{cat}) of the enzyme by dividing the rate by the enzyme concentration. The k_{cat}/K_m is what is most commonly reported. Thus, the k_{cat}/K_m can be extracted by doing an assay at a single substrate concentration (a substrate concentration at least 10x less than the K_m value).

Cys-free Glutathione Oxidation Assays

Concentration of GSSG (volume added from 100 mM stock)	0 mM (0 µL)	5 mM (25 µL)	10 mM (50 µL)	20 mM (100 µL)
Concentration of enzyme (volume added from 1 uM stock)	0.1 uM (50 µL)	0.1 uM (50 µL)	0.1 uM (50 µL)	0.1 uM (50 µL)
Volume of Assay Buffer Added	450 µL	425 µL	400 µL	350 µL
Total Reaction Volume	500 µL	500 µL	500 µL	500 µL

Table 9: This table sums up the items added to each tube for the glutathione oxidation assays on the Cys-free variants.

Each reaction was placed in a 37 °C water bath for 40 minutes. After the 40 minutes of incubation, each sample was screened for activity against paraoxon. To obtain the activities of these variants, single point kinetics are done to yield a k_{cat}/K_m value. At 0 mM, GSSG is

considered to supply the 100% activity point. The other determined activities with GSSG present are compared to the 100% activity value to obtain the percent residual activity values upon oxidation. This can be plotted against concentration of GSSG to aid in visualizing variations amongst the mutants.

Results and Discussion:

Cloning, Expression, and Purification of Variants

All variants were successfully cloned and sequence confirmed. The variants were then expressed and purified.

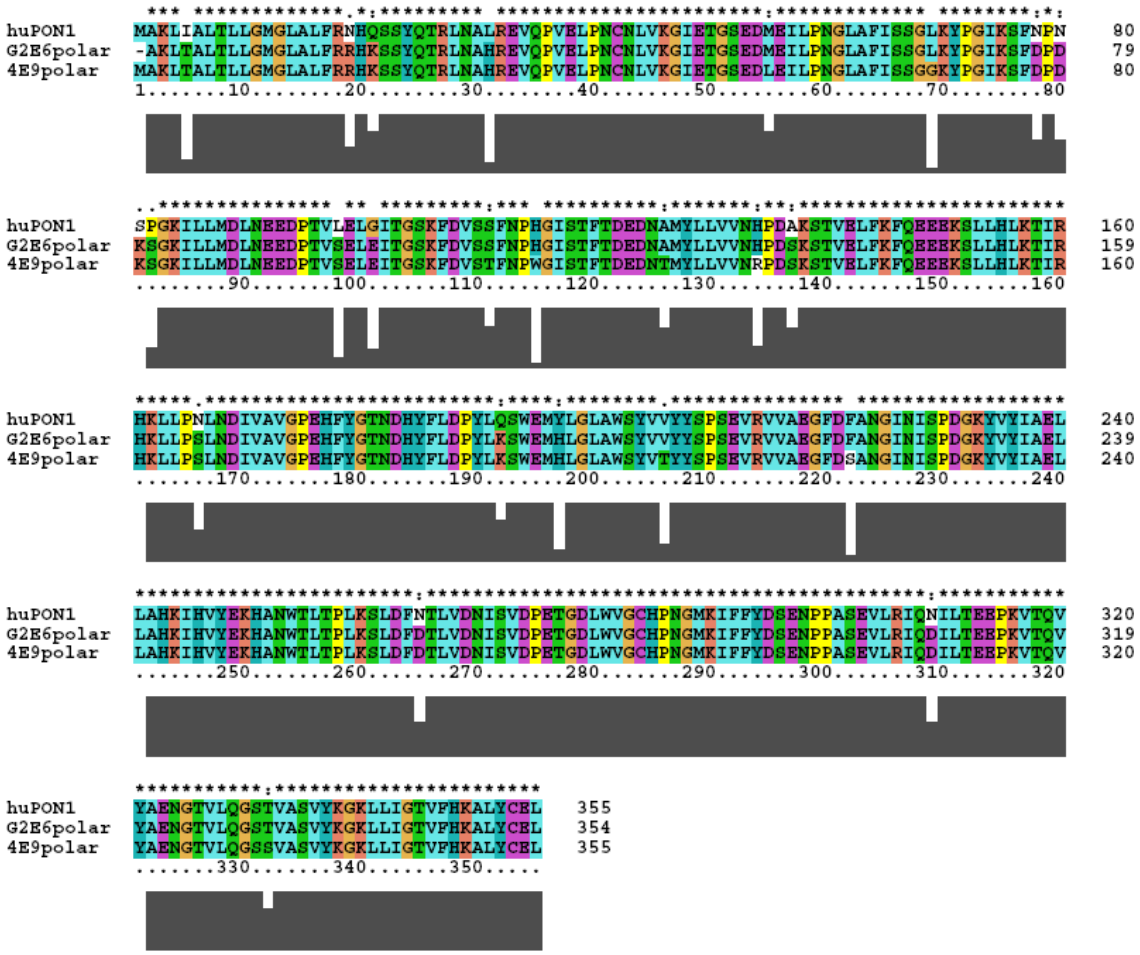

Figure 16: This is a multiple amino acid sequence alignment of huPON1, G2E6 polar, and 4E9 polar. It paints a picture of what residues were mutated from huPON1 to G2E6 polar to 4E9 polar. There are 16 mutations in G2E6p and 24 mutations in 4E9p when compared to huPON1 and only 8 mutations when compared to one another

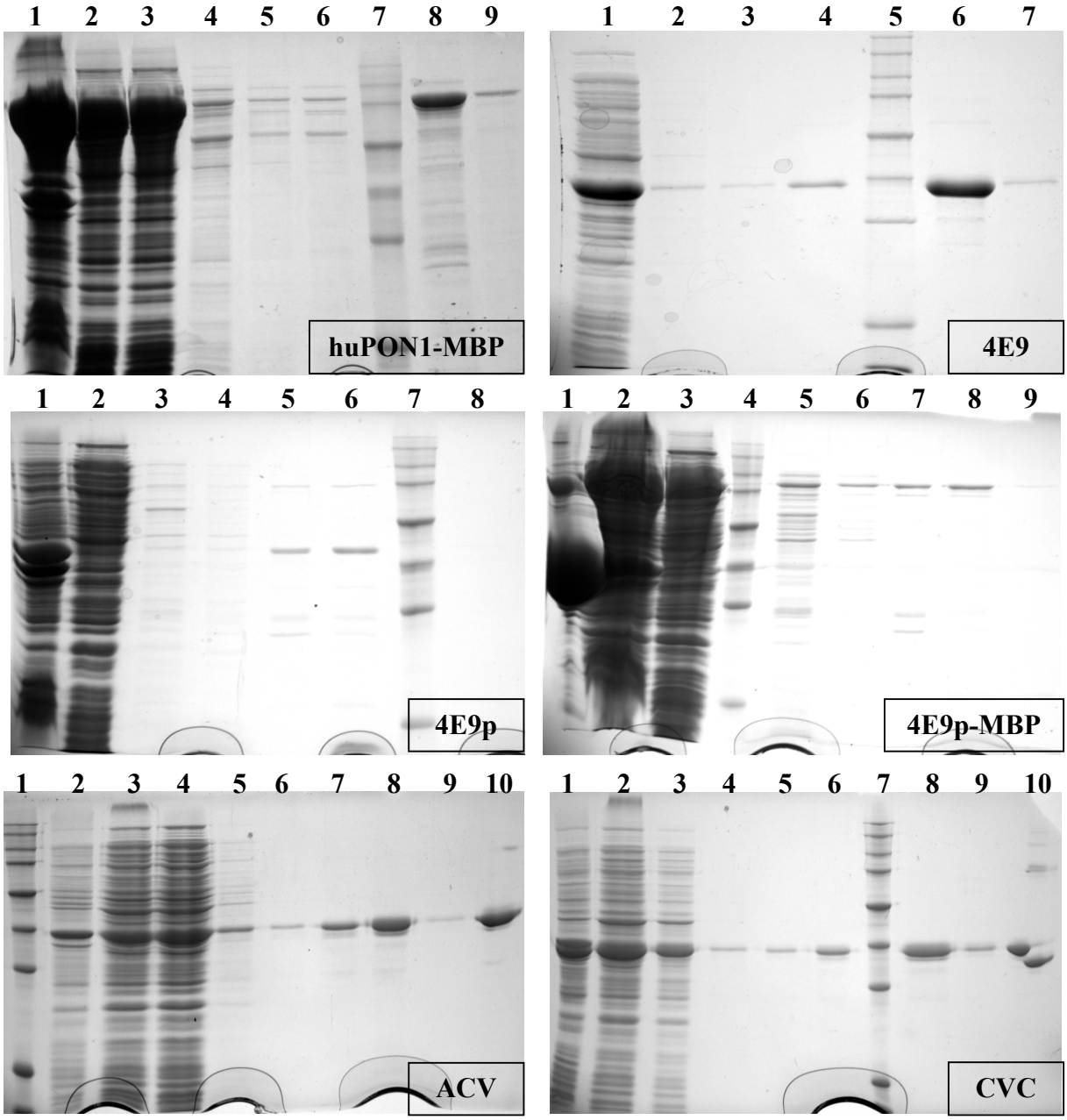

Figure 17: SDS-PAGE purification pictures for huPON1-MBP, 4E9, 4E9 polar, 4E9 polar-MBP, ACV, and CVC. All gels were 1 L preps of the samples with 10 µl of elution loaded on to gel.

Gel	Lane 1	Lane 2	Lane 3	Lane 4	Lane 5	Lane 6	Lane 7	Lane 8	Lane 9	Lane 10
Gel 1	pellet	lysate	FT	W1	W2	W3	M	E1	E2	--
Gel 2	FT	W1	W2	W3	M	E1	E2	--	--	--
Gel 3	pellet	FT	W1	W2	W3	E1	M	E2	--	--
Gel 4	pellet	lysate	FT	M	W1	W2	W3	E1	E2	--
Gel 5	M	pellet	lysate	FT	W1	W2	W3	E1	E2	E1 no DTT
Gel 6	pellet	lysate	FT	W1	W2	W3	M	E1	E2	E1 no DTT

FT-flow through, W1-wash 1, W2-wash 2, W3-wash 3, E1-elution 1, E2-elution 2, M-marker, DTT-reducing agent added to loading buffer.

The gels above give a good indication of the yield achieved from the purification of each variant. HuPON1-MBP appears to have expressed well; however, there are several bands below the product. These bands are most likely degradation product due to the hydrophobicity and instability of the protein. 4E9 yielded the highest amount of protein per liter prep. 4E9p (without MBP) did not express well, but still gives pure product. 4E9p-MBP is more soluble, as is visible in the lysate lane. Although, 4E9p (without MBP) does not express well, it is still a promising prospect because it can be purified and yield up to 4 mg of product in a 1 L prep of protein.

In the ACV and CVC gels, the last lane does not contain the reducing agent, DTT, in the loading buffer. The formation of a dimer is visible on the ACV gel. The formation of a dimer, trimer, and tetramer are visible on the CVC gel. However, based on Image J densitometry calculations, more than 90% of ACV and CVC exist in the monomeric state.

Enzyme Kinetic Data

The following table and charts summarize the kinetic data collected in the experiments as well as a Michaelis-Menten curve.

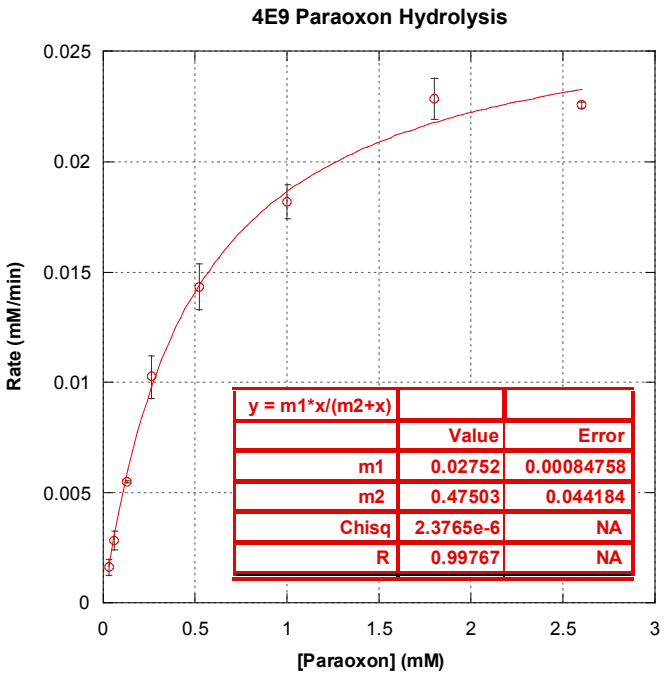

Figure 18: Michaelis-Menten plot of 4E9 when reacting with various concentrations of paraoxon (listed in **Table 6**). Error bars are also plotted and the data series is triplicated. M1 is equivalent to the V_{max} and m2 is equivalent to the K_m.

G3C9 Variants Kinetics Table *The kinetic data is listed in k_{cat}/K_m (mM^{-1} min^{-1}) with (K_m in mM)*			
Variant	**Paraoxon**	**Phenyl Acetate**	**CMP**
G3C9*	61 (2.5)	7,200 (2.4)	60 (0.15)
L69G*	15 (1.7)	62	150 (0.22)
L69S*	4.9	31	--
K70A*	33	3,800	51
F222S*	60 (0.6)	770	780 (0.04)
L240S*	12 (0.27)	730	1,140
F292A*	0.2	2,600	31.8
T332A*	47 (1.5)	2,600	9
V346A*	130 (1.3)	2,400	--

Table 10: This table gives the activities of all the G3C9 variants. All values are the k_{cat}/K_m in mM^{-1} min^{-1}. In parenthesis next to the k_{cat}/K_m is the K_m value in mM. A * indicates the data was collected by another lab member. For the G3C9 mutants, David Mata collected the phenyl acetate and paraoxon data and the results were collected at 5% constant MeOH. Christina K. Harsch collected all of the CMP data.

G3C9 Mutant Results:

All of the mutants were reduced in phenyl acetate activity and most mutants lost paraoxon activity. Two mutants, F222S and L240S, had a ten-fold increase in CMP activity. The K_m value of F222S, 0.04 mM, is much smaller than the K_m of G3C9, 0.15 mM.

Evolution of 4E9p Kinetics Table *The kinetic data is listed in k_{cat}/K_m (mM^{-1} min^{-1}) with (Km in mM)*			
Variant	**Paraoxon**	**Phenyl Acetate**	**CMP**
huPON1*	46 (0.57)	88,000 (0.66)	NSA
G2E6p MBP*	4.1	1,310	NSA
4E9p MBP	61	NSA	360 (0.04)*

Table 11: This table gives the activities of 4E9p and the variants leading to the evolution of 4E9p, G2E6p and huPON1. All values are the k_{cat}/K_m in mM^{-1} min^{-1}. In parenthesis next to the k_{cat}/K_m is the K_m value in mM. A * indicates the data was collected by another lab member. The G2E6p and huPON1 data was collected by Dr. Mohosin Sarkar. Christina K. Harsch collected all of the CMP data. NSA- No significant activity.

Cys-free 4E9 Variants Kinetics Table *The kinetic data is listed in k_{cat}/K_m (mM^{-1} min^{-1}) with (Km in mM)*			
Variant	**Paraoxon**	**Phenyl Acetate**	**CMP**
4E9	1,700 (0.47)	NSA	1,020 (0.02)*
ACV	1,250 (0.43)	NSA	880*
CVC	726 (0.37)	NSA	630*

Table 12: This table gives the activities of Cys-free 4E9 variants. All values are the k_{cat}/K_m in mM^{-1} min^{-1}. In parenthesis next to the k_{cat}/K_m is the K_m value in mM. A * indicates the data was collected by another lab member. Christina K. Harsch collected all of the CMP data. NSA- No significant activity.

4E9 Mutant Results:

4E9 had the highest activity against paraoxon and CMP amongst all of the mutants. ACV and CVC were both close to 4E9 in activity. Surprisingly, the mutant that disrupted the disulfide bond, ACV, maintained activity closer to wild-type than the mutant that disrupted the buried cysteine. This may be indicative of the buried cysteine playing a role in enzymatic

function/activity or folding/stability. Also, 4E9p is significantly more active than G3C9, huPON1, and G2E6p. All of the 4E9 mutants had no significant activity against phenyl acetate. Previous studies in lab found that the H115 position is necessary for wild-type-like phenyl acetate activity. The study mutated H115 to 10 different residues and all lost activity against phenyl acetate.[33]

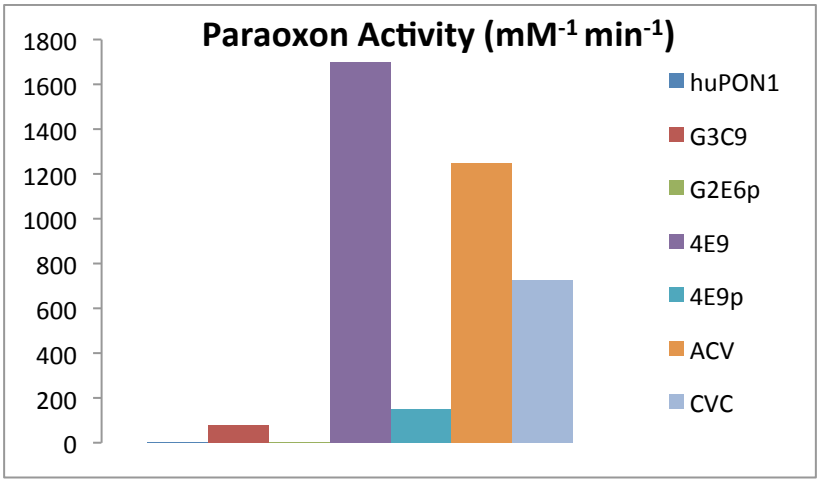

Figure 19: A bar graph comparing the activities of all the 4E9 variants (and parent molecules) that are active against paraoxon. 4E9 has the highest activity, followed by ACV, CVC, 4E9p, and G3C9. All of which have significantly higher activities than huPON1 and G2E6p.

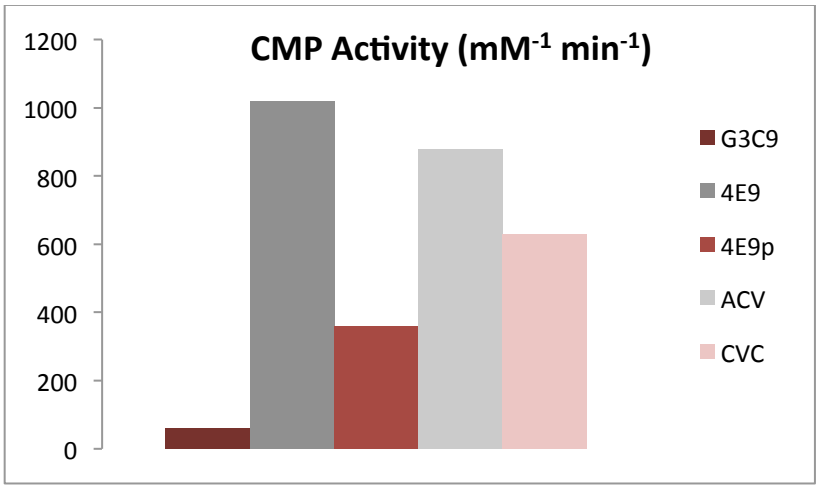

Figure 20: A bar graph comparing the activities of all the 4E9 variants (and parent molecules) that are active against CMP. 4E9 has the highest activity, followed by ACV, CVC, and 4E9p. All of which have significantly higher activities than G3C9.

Variants against S_p-isomer *The kinetic data is listed in kcat/Km (mM^{-1} min^{-1})*		
Variant	**Racemic**	**S_p-isomer**
G3C9	16	0.1
4E9	420	31
4E9polar	110	31

Table 13: This table displays the relative activities against racemic CMP and the Sp-isomer of CMP. All values are the k_{cat}/K_m in mM^{-1} min^{-1}. Christina K. Harsch collected these data points. These are relative activities at 0.025 mM CMP concentration.

Glutathione Oxidation Data

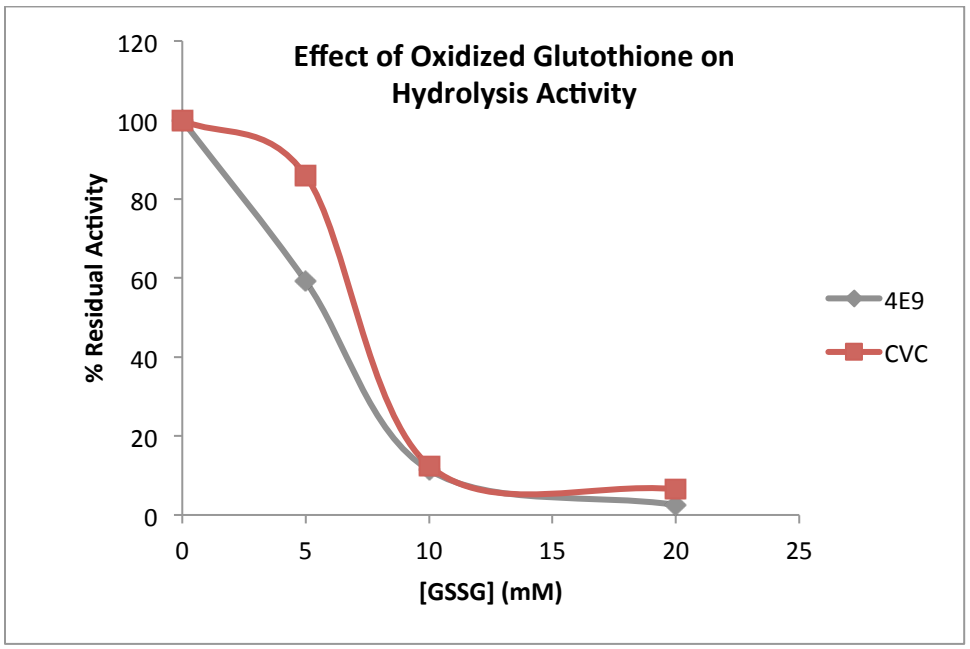

Figure 21: A graph plotting the residual activity of the Cys-free mutants versus the concentration of GSSG.

Based on the results of the glutathione oxidation experiments, CVC was better able to maintain activity under oxidizing conditions. This makes sense considering CVC contains one less cysteine. ACV is currently being tested. Thus far, the results emulate the G2E6 glutothione oxidation results.

Summary and Future Directions:

G3C9 mutagenesis helped study the active site of PON1. It aided in underlining potentially important residues for structural stability and enzymatic activity. The 4E9 Cys-free variants maintained native-like activity and CVC was more stable and less prone to activity loss under oxidizing conditions than 4E9. 4E9polar has therapeutic potential against G-agents, considering its near human primary sequence. All of the 4E9 mutants will further be studied and characterized by testing activity against G agents as well as testing in animals to determine the extent of protection against OPs. Also, thermal inactivation and melts will be done on the variants to better characterize the stability of the protein. Error prone PCR can be used on 4E9polar with aims to further enhance solubility while maintaining a human-like primary sequence.

References:

1. Dacre, J. C. (1984). Toxicology of some anticholinesterases used as chemical warfare agents – a review, in Cholinesterases, Fundamental and Applied Aspects, Brzin, M., Barnard, E. A. and Sket, D., Eds., de Gruyter, Berlin, Germany.

2. Eddleston M, Szinicz L, Eyer P, Buckley N. (2002). Oximes in acute organophosphate pesticide poisoning: a systematic review of clinical trials. *QJM*. 95 (5): 275-283.

3. Ballantyne, B. & Marrs, T. C. (1992). Overview of the biological and clinical aspects of organophosphates and carbamates, in Clinical and Experimental Toxicology of Oganophosphates and Carbamates, Ballantyne, B. & Marrs, T. C., Eds., Butterworth, Oxford, England.

4. Xie W, Stribley JA, Chatonnet A, Wilder PJ, Rizzino A, McComb RD, Taylor P, Hinrichs SH, Lockridge O. (2000); Postnatal developmental delay and supersensitivity to organophosphate in gene-targeted mice lacking acetylcholinesterase. *The Journal of Pharmacology and Experimental Therapeutic.* 293; 896-902.

5. Cherian, M. A.; Roshini, C.; Peter, J. V.; Cherian, A. M. (2005). Oximes in organophosphorus poisoning. *Indian Journal of Critical Care Medicine* (0972-5229). Vol.9, Iss.3; p.155-163

6. Weger N, Szinicz L., (1981). Therapeutic effects of new oximes, benactyzine and atropine in Soman poisoning: Part I. Effects of various oximes in Soman, Sarin, and Vx poisoning in dogs. *Fundam Appl Toxicol*. 1(2):161-3.

7. Josse, D., Xie, W., et al. (1999). Identification of residues essential for human paraoxonase (PON1) arylesterase/organophosphatase activities. *Biochemistry.* 38(9), 2816-25.

8. Masson, P.; Josse, D.; Lockridge, O.; Viguie, N.; Taupin, C.; Buhler, C., (1998). *Journal of Physiology-Paris.* 92, 357-362.

9. Amitay M, Shurki A., (2011). Hydrolysis of organophosphate compounds by mutant butyrylcholinesterase: a story of two histidines. *Proteins*. 79(2):352-64.

10. Doctor, B.P., Saxena, A., (2005). Bioscavengers for the protection of humans against organophosphate toxicity. *Chem. Biol. Interact.* 157–158, 167–171.

11. Saxena, A., Sun, W., Luo, C., Doctor, B.P., (2005). Human serum butyrylcholinesterase: in vitro and in vivo stability, pharmacokinetics, and safety in mice. *Chem. Biol. Interact.* 157–158, 199–203.

12. Saxena, A., Sun, W., Fedorko, J.M., Koplovitz, I., Doctor, B.P., (2011). Prophylaxis with human serum butyrylcholinesterase protects guinea pigs exposed to multiple lethal doses of soman or VX. *Biochem. Pharmacol.* 81, 164–169.

13. Lenz, D.E., Maxwell, D.M., Koplovitz, I., Clark, C.R., Capacio, B.R., Cerasoli, D.M., Federko, J.M., Luo, C., Saxena, A., Doctor, B.P., Olson, C., (2005). Protection against soman or VX poisoning by human butyrylcholinesterase in guinea pigs and cynomolgus monkeys. *Chem. Biol. Interact.* 157–158, 205–210.

14. Valiyaveettil M, Alamneh Y, Biggemann L, Soojhawon I, Farag HA, Agrawal P, Doctor BP, Nambiar MP., (2011). In vitro efficacy of paraoxonase 1 from multiple sources against various organophosphates. *Toxicology in Vitro.* doi:10.1016/j.tiv.2011.02.012

15. Amitay M, Shurki A., (2009); The structure of G117H mutant of butyrylcholinesterase: nerve agents scavenger. *Proteins*. 77(2):370-7.

16. Aharoni A, Gaidukov L, Yagur S, Toker L, Silman I, Tawfik DS., (2004). Directed evolution of mammalian paraoxonases PON1 and PON3 for bacterial expression and catalytic specialization. *Proc Natl Acad Sci U S A.* 101(2):482-7.

17. Harel, M., Aharoni, A., Gaidukov, L., Brumshtein, B., Khersonsky, O., Meged, R., Dvir, H., Ravelli, R.B., McCarthy, A., Toker, L., Silman, I., Sussman, J.L., Tawfik, D.S., (2004). Structure and evolution of the serum paraoxonase family of detoxifying and anti-atherosclerotic enzymes. *Nat. Struct. Mol. Biol.* 11, 412–419.

18. La Du, B.N., Billecke, S., Hsu, C., Haley, R.W., Broomfield, C.A., 2001. Serum paraoxonase (PON1) isozymes: the quantitative analysis of isozymes affecting individual sensitivity to environmental chemicals. *Drug Metab. Dispos.* 29, 566–569.

19. Costa, L.G., Cole, T.B., Furlong, C.E., (2003). Polymorphisms of paraoxonase (PON1) and their significance in clinical toxicology of organophosphates. J. *Toxicol. Clin. Toxicol*. 41, 37–45.

20. Watson, C.E., Draganov, D.I., Billecke, S.S., Bisgaier, C.L., La Du, B.N., 2001. Rabbits possess a serum paraoxonase polymorphism similar to the human Q192R. *Pharmacogenetics.* 11, 123–134.

21. Brophy, V.H., Hastings, M.D., Clendenning, J.B., Richter, R.J., Jarvik, G.P., Furlong, C.E., (2001). Polymorphisms in the human paraoxonase (PON1) promoter. *Pharmacogenetics*. 11, 77–84.

22. Ayub, A., Mackness, M.I., Arrol, S., Mackness, B., Patel, J., Durrington, P.N., (1999). Serum paraoxonase after myocardial infarction. Arterioscler. Thromb. Vasc. *Biol*. 19, 330–335.

23. Costa, L.G., Cole, T.B., Furlong, C.E., (2005). Paraoxonase (PON1): from toxicology to cardiovascular medicine. *Acta Biomed.* 76 (suppl.2), 50–57.

24. Mackness, B., Durrington, P.N., Mackness, M.I., (2002). The paraoxonase gene family and coronary heart disease. *Curr. Opin. Lipidol.* 13, 357–362.

25. La Du, B. N., Aviram, M., Billecke, S., Navab, M., Primo-Parmo, S., Sorenson, R. C. & Standiford, T. J. (1999). On the physiological role(s) of the paraoxonases. *Chem Biol Interact.* 119-120, 379-388.

26. Yeung, D. T., Josse, D., Nicholson, J. D., Khanal, A., McAndrew, C. W., Bahnson, B. J., Lenz, D. E. & Cerasoli, D. M. (2004). Structure/function analyses of human serum paraoxonase (HuPON1) mutants designed from a DFPase-like homology model. *Biochem Biophys Acta*. 1702, 67-77.

27. Kapust, R.B. & Waugh, D.S. (1999). Escherichia coli maltose-binding protein is uncommonly effective at promoting the solubility of polypeptides to which it is fused. *Protein Sci.* 8, 1668-1674.

28. Sarkar, M. (2010). Engineering Proteins with GFP: Study of Protein-Protein Interactions In Vivo, Protein Expression and Solubility. *Ph. D Dissertation,* The Ohio State University.

29. Gupta RD, Goldsmith M, Ashani Y, Simo Y, Mullokandov G, Bar H, Ben-David M, Leader H, Margalit R, Silman I, Sussman JL, Tawfik DS. (2011). Directed evolution of hydrolases for prevention of G-type nerve agent intoxication. *Nat Chem Biol.* 7(2):120-5.

30. Hari SB, Byeon C, Lavinder JJ, Magliery TJ. (2010). Cysteine-free Rop: a four-helix bundle core mutant has wild-type stability and structure but dramatically different unfolding kinetics. *Protein Sci.* (4): 670-9

31. Sayre R, Wang G, Magliery TJ. Paraoxonase-1 NIH- U54NS0581183 Research Grant Proposal for Project 6.

32. Shete V, Competty B, Magliery TJ. (2011). Unpublished results.

33. Mata DM, Harsch CK, Bharwani N, Magliery TJ. (2011). Unpublished results.